

# Analysis of Turbulent Particle Fluxes in Reduced MHD Simulation

Haruhiko TODOROKI<sup>1)</sup>, Naohiro KASUYA<sup>1,2)</sup> and Masatoshi YAGI<sup>3)</sup>

<sup>1)</sup>Interdisciplinary Graduate School of Engineering Sciences, Kyushu University, Kasuga, Fukuoka 816-8580, Japan

<sup>2)</sup>Research Institute for Applied Mechanics, Kyushu University, Kasuga, Fukuoka 816-8580, Japan

<sup>3)</sup>National Institutes for Quantum Science and Technology, Rokkasho, Aomori 039-3212, Japan

(Received 19 February 2023 / Accepted 8 May 2023)

Some local turbulence analyses in tokamaks have shown that inward particle fluxes are induced in inversed density gradient regions. To evaluate the particle transport effect, we carry out global simulations using a 5-field reduced MHD model with an inversed density gradient near the plasma edge. Outward particle fluxes in the steeper gradient region are dominant, which mainly determine the evolution of the density profile. On the other hand, inward particle fluxes are also induced in the inversed gradient region. The electron drift modes are possible to become unstable with negative density gradients. The contribution of the inward particle fluxes is found to be present and its fraction is increased with nonlinear excitation of low  $n$  modes in the nonlinear phase, where  $n$  is the toroidal mode number.

© 2023 The Japan Society of Plasma Science and Nuclear Fusion Research

Keywords: particle pinch effect, tokamak, turbulence, reduced MHD model

DOI: 10.1585/pfr.18.1203052

Fueling to the core plasma by inward particle fluxes is one of the key issues to maintain a high fusion reaction rate in magnetically-confined plasmas [1]. There are many theories for turbulent particle pinch for normal density and temperature gradient cases [2–5]. A high-density region is created near the plasma edge due to ablation by pellet injection, resulting in a hump-shaped density profile with an inversed gradient in the radial direction. The inversed density gradient is known to produce the inward particle flux [6]. In order to elucidate the mechanism of the inward particle flux, which is effective in fueling to the plasma center, we perform global turbulence simulations by using a reduced MHD model to evaluate particle convective transport, when an inversed density gradient is introduced into tokamak plasmas.

R5F code is used for simulations which is a global simulation code using the following reduced MHD model with neoclassical viscous effects [7];

$$\begin{aligned} \frac{d}{dt} \nabla_{\perp}^2 \left( \phi + \frac{\beta_i}{\beta} p \right) &= -\nabla_{\parallel} \nabla_{\perp}^2 A - [2r \cos \theta, T_e N] \\ &\quad + \mu_{i\perp} \nabla_{\perp}^4 \left( \phi + \frac{\beta_i}{\beta} p \right) \\ &\quad - \frac{q}{\varepsilon} \mu_i \frac{1}{r} \frac{\partial}{\partial r} (r U_i) \\ &\quad - \frac{q}{\varepsilon} \frac{m_e}{m_i} \mu_e \frac{1}{r} \frac{\partial}{\partial r} (r U_e), \end{aligned} \quad (1)$$

$$\begin{aligned} \frac{\partial A}{\partial t} - \delta^2 \frac{m_e}{m_i} \frac{d}{dt} \nabla_{\perp}^2 A &= -\nabla_{\parallel} (\phi - \delta T_e N) + \eta_{\parallel} \nabla_{\perp}^2 A \\ &\quad - 4\mu_{e\perp} \delta^2 \frac{m_e}{m_i} \nabla_{\perp}^4 A \\ &\quad + \delta \frac{m_e}{m_i} \mu_e U_e + \alpha_T \delta \nabla_{\parallel} T_e, \end{aligned} \quad (2)$$

$$\frac{dV}{dt} = -\nabla_{\parallel} (T_e N) + 4\mu_{i\perp} \nabla_{\perp}^2 V - \mu_i U_i - \frac{m_e}{m_i} \mu_e U_e, \quad (3)$$

$$\begin{aligned} (1 + \beta) \frac{dN}{dt} + \beta \frac{dT_e}{dt} &= -\beta \nabla_{\parallel} (V + \delta \nabla_{\perp}^2 A) \\ &\quad + \eta_{\perp} \beta \nabla_{\perp}^2 (T_e N) \\ &\quad + \beta [2r \cos \theta, \phi - \delta T_e N], \end{aligned} \quad (4)$$

$$\begin{aligned} \frac{3}{2} \frac{dT_e}{dt} - \frac{\beta_e}{\beta} \frac{dN}{dt} &= -\alpha_T \delta \beta_e \nabla_{\parallel} \nabla_{\perp}^2 A + \varepsilon^2 \chi_{e\parallel} \nabla_{\parallel}^2 T_e \\ &\quad + \chi_{e\perp} \nabla_{\perp}^2 T_e \\ &\quad - \frac{5}{2} \delta \beta_e [2r \cos \theta, T_e]. \end{aligned} \quad (5)$$

The definitions of the quantities are written in Ref. [7]. In this code, time evolutions of five variables, electrostatic potential  $\phi$ , vector potential parallel to the magnetic field  $A$ , parallel velocity  $V$ , electron density  $N$ , electron temperature  $T_e$  are solved in the 3-D space. The following tokamak plasma parameters are used for the simulations; major radius  $R = 1.5$  m, minor radius  $a = 0.5$  m, plasma beta  $\beta = 1 \times 10^{-2}$ , normalized ion skin depth  $\delta = 1 \times 10^{-2}$ . The inversed density gradient near the plasma edge due to pellet injection is modeled by giving the initial condition of the background density profile at  $t = 0$  with source peak height  $S_{\text{amp}}$  (density intensity) and width  $\Delta$  at radial position  $r = r_s$  as  $N(t = 0) = N_0 \left( (1 - r^\alpha)^\alpha + S_{\text{amp}} \exp \left( -(r - r_s)^2 / (2\Delta^2) \right) \right)$ , where  $r$  is normalized by  $a$ . We call the region of positive and negative density gradients near the position  $r = r_s$  inversed and normal gradient regions, respectively.

In this study, we analyze the case with  $S_{\text{amp}} = 1.5$  and  $r_s = 0.8$ . Figure 1 shows the time evolution of the density profile and the internal energy of each mode, where  $n$

author's e-mail: todoroki@riam.kyushu-u.ac.jp

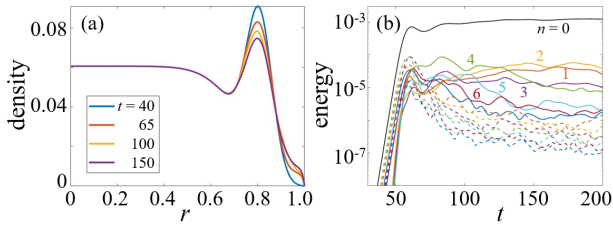


Fig. 1 Time evolution of (a) a density profile and (b) internal energy of each mode in R5F calculation with  $S_{\text{amp}} = 1.5$ .

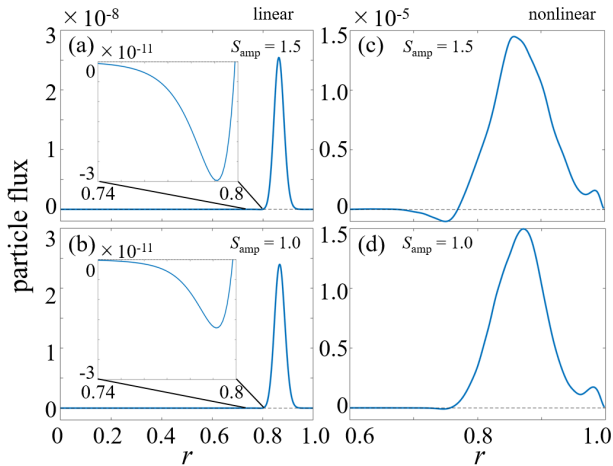


Fig. 2 Radial profiles of the particle flux in the linear phase with  $S_{\text{amp}} =$  (a) 1.5 ( $t = 40$ ) and (b) 1.0 ( $t = 67$ ), and in the nonlinear phase with  $S_{\text{amp}} =$  (c) 1.5 ( $t = 100$ ) and (d) 1.0 ( $t = 111$ ). The magnifications in the inversed gradient region in the linear phase are also shown.

is the toroidal mode number. From Fig. 1 (a), the density peak height becomes smaller in time with outward transport induced by the resistive ballooning mode in the normal gradient region. In the linear phase, components with  $n = 8 - 11$  are dominantly excited in the normal gradient region, while in the nonlinear phase they are saturated with the background profile relaxation by themselves. The fluctuation amplitudes are much larger in the normal gradient region than in the inversed gradient region, which mainly determine the particle transport.

The direction and magnitude of the particle fluxes are evaluated in the time evolution. Figure 2 shows the radial profiles of the particle flux in the linear and nonlinear phases. The  $n = 8$  component, which is strongly excited in the normal gradient region, is dominant overall to drive an outward particle flux. On the other hand, there is a contributor to induce an inward particle flux in the inversed gradient region as in Fig. 2. The magnification in Fig. 2 (a) shows that in the linear phase the magnitude is much smaller than the magnitude of the outward flux in the normal gradient region. We also calculate a smaller gradient case with  $S_{\text{amp}} = 1.0$ , which shows the peak magnitude of the inward particle flux in the inversed gradient region has almost the

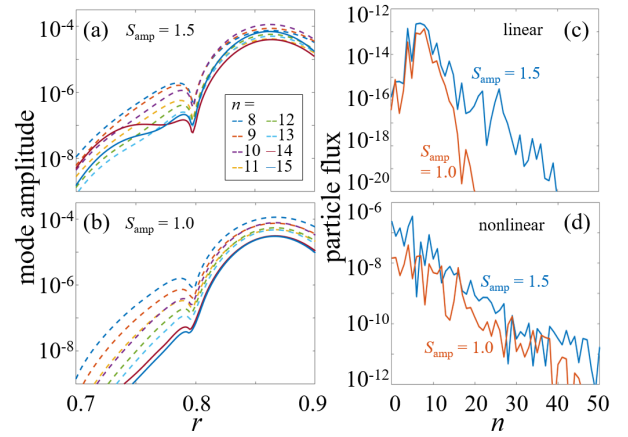


Fig. 3 (a) Radial profiles of mode amplitude decomposed into each toroidal mode component in the linear phase with  $S_{\text{amp}} =$  (a) 1.5 and (b) 1.0. Comparison of the particle fluxes from each toroidal mode component in the (c) linear phase and (d) nonlinear phase at the inversed gradient region ( $r = 0.75$ ).

same level as in Fig. 2 (b). However, the magnitude is different in the nonlinear phase as in Figs. 2 (c) and 2 (d). The ratio  $\Gamma_{\text{peak\_in}} / \Gamma_{\text{peak\_out}}$  is 0.07% and 10% with  $S_{\text{amp}} = 1.0$  and  $S_{\text{amp}} = 1.5$ , where  $\Gamma_{\text{peak\_in}}$  and  $\Gamma_{\text{peak\_out}}$  is the peak magnitude of the particle flux in the inversed and normal gradient regions, respectively. With  $S_{\text{amp}} = 1.5$ , the inward particle flux in the inversed gradient region becomes larger, and is sustained in the nonlinear phase.

The inward particle flux is possibly driven by the resistive electron drift wave unstable in the inversed gradient region. The linear growth rate is calculated using the local model of the electron drift mode [6]. The modes are unstable with the parameters used in the R5F simulations, and the larger density gradient (smaller  $|L_n|$ ) gives the larger linear growthrate (10% larger with  $S_{\text{amp}} = 1.5$  than  $S_{\text{amp}} = 1.0$ ). Actually, the global simulations show that the  $n = 14$  component has larger magnitude for  $S_{\text{amp}} = 1.5$  (Fig. 3 (a)), though is small for  $S_{\text{amp}} = 1.0$  (Fig. 3 (b)) in the inversed gradient region ( $r = 0.7 - 0.8$ ). Comparison of the particle fluxes from each toroidal mode component in the linear phase (Fig. 3 (c)) shows excitation of high  $n$  components for the  $S_{\text{amp}} = 1.5$  case. This result is possible to be related with the dependency of the linear growthrate. On the other hand, the mechanism to sustain the larger flux in the nonlinear phase with  $S_{\text{amp}} = 1.5$  is related to nonlinear excitation of low  $n$  modes. Comparison of the particle fluxes from each toroidal mode component in the nonlinear phase (Fig. 3 (d)) shows larger contribution of  $n = 0 - 5$  modes, which are excited nonlinearly, for the  $S_{\text{amp}} = 1.5$  case. Inverse cascade of the mode energy is the key for the sustainment of the relatively large inward particle flux.

In this way the global reduced MHD code was used to evaluate turbulent particle transport with an inversed density gradient near the plasma edge. Outward particle fluxes

in the normal gradient region are dominant, but inward particle fluxes are also induced in the inversed gradient region. The magnitude of the inward fluxes is increased with a larger density gradient. The electron drift mode is possible to become unstable, but is found to have rather small effect on particle transport, so the ion mixing mode [2] or ion temperature gradient mode with trapped electron response should be investigated in the near future.

This work was partially supported by JSPS KAKENHI JP20K03905, and the collaboration program of RIAM in Kyushu University. Some calculations were carried out using JFRS-1 supercomputer system at

IFERC-CSC in QST.

- [1] C. Angioni *et al.*, Plasma Phys. Control. Fusion **51**, 124017 (2009).
- [2] B. Coppi and C. Spight, Phys. Rev. Lett. **41**, 551 (1978).
- [3] G.S. Lee and P.H. Diamond, Phys. Fluids **29**, 3291 (1986).
- [4] R.E. Waltz and R.R. Dominguez, Phys. Fluids B **1**, 1935 (1989).
- [5] X. Garbet *et al.*, Phys. Rev. Lett. **91**, 035001 (2003).
- [6] M. Yagi *et al.*, Proc. BPSI Meeting, 2-1 (2018). [https://www.riam.kyushu-u.ac.jp/sosei/bpsi/2018/BPSI2018\\_proc.pdf](https://www.riam.kyushu-u.ac.jp/sosei/bpsi/2018/BPSI2018_proc.pdf)
- [7] M. Yagi *et al.*, 26th IAEA FEC, TH/P3-21 (2016).